Proceedings of the 2020 Dynamic Systems and Control (DSC) Conference
DSCC 2020
October 4-7, 2020, Pittsburgh, USA

DSCC2020-3257

VIBRATIONAL CONTROL OF A 2-LINK MECHANISM

Zakia Ahmed *
Department of Mechanical Engineering
Virginia Tech
Blacksburg, Virginia, 24061
Email: zakiaahmed@vt.edu

Sevak Tahmasian
Department of Biomedical
Engineering and Mechanics
Virginia Tech
Blacksburg, Virginia, 24061
Email: sevakt@vt.edu

Craig A. Woolsey
Department of Aerospace and
Ocean Engineering
Virginia Tech
Blacksburg, Virginia, 24061
Email: cwoolsey@vt.edu

ABSTRACT

This paper describes vibrational control and stability of a planar, horizontal 2-link mechanism using translational control of the base pivot. The system is a 3-DOF two-link mechanism that is subject to torsional damping, torsional stiffness, and is moving on a horizontal plane. The goal is to drive the averaged dynamics of the system to a desired configuration using a high-frequency, high-amplitude force applied at the base pivot. The desired configuration is achieved by applying an amplitude and angle of the input determined using the averaged dynamics of the system. We find the range of stable configurations that can be achieved by the system by changing the amplitude of the oscillations for a fixed input angle and oscillation frequency. The effects of varying the physical parameters on the achievable stable configurations are studied. Stability analysis of the system is performed using two methods: the averaged dynamics and averaged potential.

INTRODUCTION

Vibrational control of mechanical systems is an open-loop control strategy that applies a high frequency, high amplitude input to stabilize the system about a desired state or trajectory. The desired configuration of the system may be a previously unstable equilibrium that is stabilized using the vibrational input. An advantage of applying vibrational control is that it is an open-loop control strategy which can be useful in underactuated systems with unmeasurable states or where measuring a state may be difficult or expensive.

Vibrational control theory was discussed by Meerkov in [1] where he developed the necessary and sufficient conditions for vibrational stabilizability of linear dynamic systems. Bellman, Bentsman, and Meerkov, in [2, 3], expanded on the work in [1] by applying vibrational control to nonlinear systems. Vibrational control systems use high-frequency, high-amplitude force or moment. The analysis of dynamics with high-frequency time-periodic inputs is made simpler using averaging techniques [4–6]. Bullo [7, 8] developed an averaging technique applied to a class of mechanical control systems with high-frequency, high-amplitude inputs, which is used in this paper; the method requires forcing at a "sufficiently high" frequency, although determining this minimum frequency can be difficult. Tahmasian and Woolsey developed a control design method for underactuated mechanical systems and applied vibrational control to a 3-DOF system with two oscillatory inputs [9,10]. Higher order averaging is explored by Vela, Morgansen, and Burdick in [11, 12] in applications such as biomimetic locomotion. Berg and Wickramasinghe developed a method for vibrational control without averaging using stability maps for second order linear periodic systems in [13]; their work illustrates and then circumvents the problem of determining a lower bound for the forcing frequency. Baillieul introduced the use of an "averaged potential" in [14] for stability analysis of periodically forced systems. Weibel and Baillieul used the "averaged potential" and averaging methods for robust open-loop control in [15].

While vibrational control is a fascinating illustration of non-

*Address all correspondence to this author.

intuitive mechanical system behavior, it also has a variety of applications. Wickramasinghe and Berg used vibrational control to delay the onset of the pull-in instability for an electrostatic comb drive [16]. Taha, Kiani, and Navarro discussed the application of vibrational control in flapping-wing micro-air-vehicles [17]. Guo, Wang, Qu, and Braiman used open-loop vibrational control for atomic-scale friction control in a friction force microscope [18]. Blekhman describes applications of vibrational mechanics such as the vibro-flier and vibro-ships in [19], as well as some clever material transport strategies. The vibro-flier is an apparatus that is lifted upwards due to axial oscillations of a body. Vibro-ships experience transport due to the presence of fins and the action of random hydrodynamic forcing from a fluid.

In this paper, we use the averaging technique developed in [7, 8] to study the dynamics of a 3-DOF planar, horizontal 2-link mechanism with an applied force at the base pivot. The system is subject to linear torsional damping and linear torsional stiffness and its motion is not affected by gravity. The goal is to drive the system to a neighborhood of a desired configuration using the oscillatory input amplitude and angle. The achievable stable configurations of the system are presented and the effects of variation of the physical parameters on the achievable stable configurations are studied. Additionally, stability analysis is performed using the averaged potential described in [15]. Performing stability analysis using the averaged dynamics and averaged potential prompt the following questions:

1. Do the conditions for stability obtained using these two perspectives agree?
2. If the conditions do not agree, which perspective provides the least conservative conditions?

The paper continues with a brief discussion of averaging, followed by modeling details for the apparatus that we consider. We then present a numerical investigation of the stable equilibria for the period-averaged, vibrationally forced mechanism followed by formal stability analysis.

AVERAGING

Consider the following system in the form of an initial value problem:

$$\dot{\mathbf{x}} = \varepsilon \mathbf{f}(\mathbf{x}, t), \qquad \mathbf{x}(0) = \mathbf{x}_0 \tag{1}$$

where $\mathbf{f}(\mathbf{x}, t)$ is a T-periodic function in its second argument and $\varepsilon > 0$ is a small number. The time-averaged dynamics of the system (1) is defined as [7]

$$\dot{\bar{\mathbf{x}}} = \varepsilon \bar{\mathbf{f}}(\bar{\mathbf{x}}), \qquad \bar{\mathbf{x}}(0) = \mathbf{x}_0 \tag{2}$$

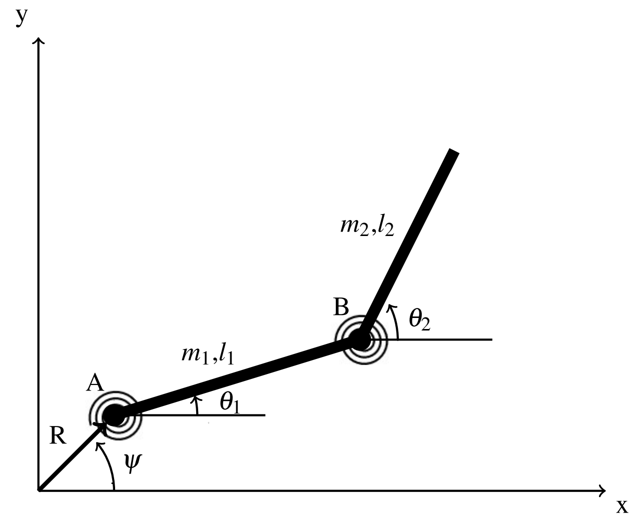

FIGURE 1: A 3-DOF PLANAR, HORIZONTAL 2-LINK MECHANISM WITH PIVOT AT A CONSTRAINED TO MOVE RADIALLY FROM THE ORIGIN AT AN ANGLE ψ.

where

$$\bar{\mathbf{f}}(\bar{\mathbf{x}}) = \frac{1}{T}\int_0^T \mathbf{f}(\bar{\mathbf{x}}, t)dt \tag{3}$$

Theorem 1 *(First order periodic averaging [8]): There exists a positive ε_0 such that, for all $0 < \varepsilon \le \varepsilon_0$,*

(i) $\mathbf{x}(t) - \bar{\mathbf{x}}(t) = O(\varepsilon)$ *as* $\varepsilon \to 0$ *on the time scale* $1/\varepsilon$*, and*
(ii) *if the origin is an exponentially stable equilibrium of (2), then there is a corresponding exponentially stable periodic orbit of (1).*

Next, consider an n-DOF mechanical control system whose dynamics are written in first-order form:

$$\dot{\mathbf{x}} = \mathbf{Z}(\mathbf{x}) + \sum_{i=1}^{m} \mathbf{Y}_i(\mathbf{x}) \left(\frac{1}{\varepsilon}\right) v_i\left(\frac{t}{\varepsilon}\right), \qquad \mathbf{x}(0) = \mathbf{x}_0 \tag{4}$$

where $\mathbf{x}$ is the state vector (i.e., the vector of configurations and velocities), $\mathbf{Z}(\mathbf{x})$ is the drift vector field, $\mathbf{Y}_i(\mathbf{x})$, $i \in \{1, ..., m | m \le n\}$, are the input vector fields for the force (or moment) inputs, ε is a small, positive number, and $v_i(t)$ is a zero-mean T-periodic input function. Associated with the input functions we define scalar parameters κ_i, Λ_{ij}, and μ_{ij} for $i, j \in \{1, ..., m\}$ as follows [20]

$$\kappa_i = \frac{1}{T}\int_0^T \int_0^t v_i(\tau) d\tau\, dt \tag{5}$$

$$\Lambda_{ij} = \frac{1}{T}\int_0^T \left(\int_0^t v_i(\tau)d\tau\right)\left(\int_0^t v_j(\tau)d\tau\right)dt \tag{6}$$

and

$$\mu_{ij} = \frac{1}{2}\left(\Lambda_{ij} - \kappa_i\kappa_j\right) \tag{7}$$

We define the *symmetric product* between two input vector fields $\mathbf{Y}_i(\mathbf{x})$ and $\mathbf{Y}_j(\mathbf{x})$ as

$$\langle \mathbf{Y}_i : \mathbf{Y}_j\rangle(\mathbf{x}) = \langle \mathbf{Y}_j : \mathbf{Y}_i\rangle(\mathbf{x}) = [\mathbf{Y}_j(\mathbf{x}), [\mathbf{Z}(\mathbf{x}), \mathbf{Y}_i(\mathbf{x})]] \tag{8}$$

where $[\cdot,\cdot]$ denotes the Lie bracket of the vector fields [10].

Theorem 2 *(Averaging of systems subject to oscillatory inputs [8], [20]): Given the system (4) with high-amplitude, high-frequency T-periodic inputs $\frac{1}{\varepsilon}v_i(\frac{t}{\varepsilon})$. Suppose the components of $\mathbf{Z}(\mathbf{x})$ are homogeneous polynomials of velocities of degree two or less. Consider the time-invariant system*

$$\dot{\bar{\mathbf{x}}} = \mathbf{Z}(\bar{\mathbf{x}}) - \sum_{i,j=1}^{m} \mu_{ij}\langle \mathbf{Y}_i : \mathbf{Y}_j\rangle(\bar{\mathbf{x}}) \tag{9}$$

with the initial conditions $\bar{\mathbf{x}}(0) = \bar{\mathbf{x}}_0$. Then there exists a positive ε_0 such that, for all $0 < \varepsilon \le \varepsilon_0$, $\mathbf{x}(t) - \bar{\mathbf{x}}(t) = O(\varepsilon)$ as $\varepsilon \to 0$ on the time scale $1/\varepsilon$. If the system (9) has an exponentially stable equilibrium point, then the system (4) has a corresponding exponentially stable periodic orbit for all $t \ge 0$.

The time-invariant system (9) is referred to as the averaged form, or averaged dynamics, of the time-periodic system (4).

A PLANAR, HORIZONTAL 2-LINK MECHANISM

Consider the 3-DOF planar, horizontal 2-link mechanism as depicted in Fig. 1. The system consists of two links of masses m_1 and m_2 and lengths l_1 and l_2, respectively. The links move on a horizontal plane, i.e. their motions are not affected by gravity. The base pivot of the first link, joint A, is constrained to move radially from the origin, at an angle ψ measured counter-clockwise from the positive x-axis. The distance from the origin to the base pivot for this prescribed radial motion is $R = r\varepsilon\cos\left(\frac{t}{\varepsilon}\right)$. Joint A has a torsional stiffness k_{t_1} and torsional damping coefficient k_{d_1}. Joint B connects the two links l_1 and l_2 and has a torsional stiffness k_{t_2} and torsional damping coefficient k_{d_2}. The torsional stiffness and damping resist the rotation of the links.

Vibrational Control of the 2-link Mechanism

The goal of this section is to control the orientation of the two links using an oscillatory displacement input applied to joint A to achieve desired orientation angles of the two links. The dynamic equations of the system are:

$$\mathbf{M}(\mathbf{q})\ddot{\mathbf{q}} + \mathbf{g}(\mathbf{q},\dot{\mathbf{q}}) = \mathbf{h}(\mathbf{q})\mathbf{u}(t) \tag{10}$$

where $\mathbf{q} = (\theta_1, \theta_2)^T$, the inertia matrix is

$$\mathbf{M}(\mathbf{q}) = \begin{pmatrix} m_1d_1^2 + I_1 + m_2l_1^2 & m_2d_2l_1\cos(\theta_1-\theta_2) \\ m_2d_2l_1\cos(\theta_1-\theta_2) & I_2 + m_2d_2^2 \end{pmatrix},$$

$$\mathbf{g}(\mathbf{q},\dot{\mathbf{q}}) = \begin{pmatrix} k_{d_1}\dot{\theta}_1 + k_{d_2}\left(\dot{\theta}_1 - \dot{\theta}_2\right) + m_2d_2l_1\sin(\theta_1-\theta_2)\dot{\theta}_2^2 + k_{t_1}\theta_1 + k_{t_2}(\theta_1-\theta_2) \\ k_{d_2}\left(\dot{\theta}_2 - \dot{\theta}_1\right) - m_2d_2l_1\sin(\theta_1-\theta_2)\dot{\theta}_1^2 + k_{t_2}(\theta_2-\theta_1) \end{pmatrix},$$

$$\mathbf{h}(\mathbf{q}) = \begin{pmatrix} (m_1d_1+m_2l_1)\sin\theta_1 & -(m_1d_1+m_2l_1)\cos\theta_1 \\ m_2d_2\sin\theta_2 & -m_2d_2\cos\theta_2 \end{pmatrix},$$

and

$$\mathbf{u}(t) = \begin{pmatrix} \ddot{x}(t) \\ \ddot{y}(t) \end{pmatrix}$$

where d_1 and d_2 are the distances from joints A and B to the centers of mass of links 1 and 2, respectively. I_1 and I_2 are the mass moments of inertia about the centers of mass of links 1 and 2, respectively. The acceleration components $\ddot{x}$ and $\ddot{y}$ are defined by the prescribed pivot motion

$$x(t) = r\varepsilon \cos\left(\frac{\omega_0 t}{\varepsilon}\right) \cos\psi \tag{11a}$$

$$y(t) = r\varepsilon \cos\left(\frac{\omega_0 t}{\varepsilon}\right) \sin\psi \tag{11b}$$

where $r\varepsilon$ is the amplitude and $\frac{\omega_0}{\varepsilon}$ is the frequency of oscillation. (In the following, we substitute the value $\omega_0 = 1$ rad/s.) The displacement input is a time-periodic zero-mean function (in this example it is the cosine function) that moves the endpoint A of link 1 back and forth at a prescribed angle ψ that is measured counterclockwise from the positive x-axis.

The dynamic equations of the system (10) can be written in the form of (4) where the drift vector field is

$$\mathbf{Z}(\mathbf{x}) = \begin{pmatrix} \dot{\mathbf{q}} \\ -\mathbf{M}^{-1}(\mathbf{q})\mathbf{g}(\mathbf{q},\dot{\mathbf{q}}) \end{pmatrix}$$

and the periodic forcing that acts on the system is

$$\mathbf{Y}(\mathbf{x})\frac{1}{\varepsilon}v\left(\frac{t}{\varepsilon}\right) = \frac{1}{\varepsilon}\begin{pmatrix} \mathbf{0}_{2\times 1} \\ \mathbf{M}^{-1}(\mathbf{q})\mathbf{h}(\mathbf{q}) \end{pmatrix} \cos\left(\frac{t}{\varepsilon}\right)$$

The drift and input vector fields are then used to obtain the averaged dynamics of the system, as shown in (9). To control the orientation of the links, a desired configuration, $\theta_e = (\theta_{1e}, \theta_{2e})$, is prescribed. The desired configuration is used to obtain solutions for the amplitude of the displacement input, $r\varepsilon$, and the direction of the displacement ψ. The input frequency (as determined by the non-dimensional parameter ε) is prescribed, so the problem is to solve for the parameter r. If the desired configuration is achievable, there will be one pair of real solutions, only one of which will be admissible. The admissible solutions will be referred to as r_e and ψ_e.

If θ_e can be achieved, the next step is to assess the stability of this configuration. Our aim is to implement vibrational control on an experimental apparatus matching the model described here. In order for a desired configuration to be observed in this experiment, the desired configuration must be a stable equilibrium point of the averaged dynamics. To determine stability, the Jacobian matrix of the averaged dynamics is found for θ_e, r_e, and ψ_e . If the eigenvalues of this matrix have negative real parts then the configuration will be locally asymptotically stable. Figure 2 shows the actual and averaged time histories of the link angles for a stable desired configuration of $\theta_e = (-\frac{\pi}{18}, \frac{\pi}{9})^T$ radians. The parameter $\varepsilon = 1/70$. The required value of r and input angle ψ were calculated to be $r_e = 1.74$ m/s and $\psi_e = 1.64$ radians, respectively. The initial conditions are $\theta_0 = (\theta_{1_0}, \theta_{2_0})^T = (\frac{\pi}{18}, \frac{5\pi}{18})$ radians. The physical parameters used to characterize the system are presented in Table 1.

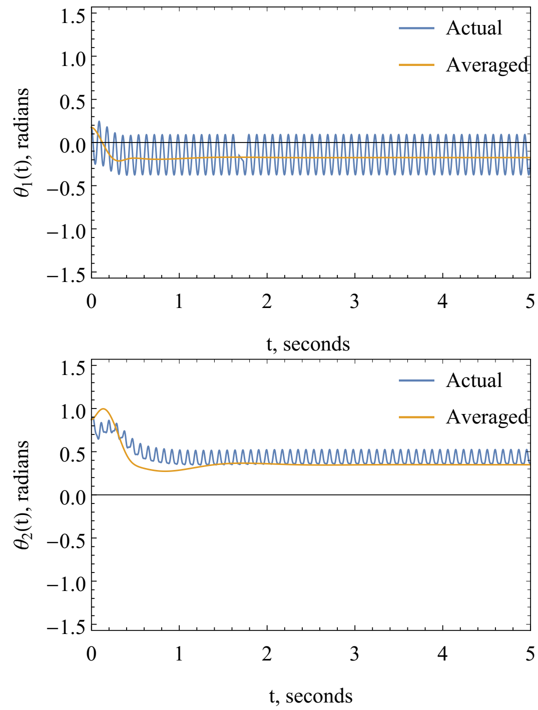

FIGURE 2: TIME HISTORIES OF θ_1 AND θ_2 TO ACHIEVE THE DESIRED CONFIGURATION $\theta_e = (-\frac{\pi}{18}, \frac{\pi}{9})$ RADIANS, $r_e = 1.74$ M/S, AND $\psi_e = 1.64$ RADIANS.

TABLE 1: PHYSICAL PARAMETERS OF THE SYSTEM.

Parameter	Value
m_1	0.081 kg
m_2	0.0675 kg
l_1	0.12 m
l_2	0.10 m
k_{t_1}	0.25 N-m/rad
k_{t_2}	0 N-m/rad
k_{d_1}	0.003 N-m/(rad/s)
k_{d_2}	0.002 N-m/(rad/s)

STABLE CONFIGURATIONS OF THE 2-LINK MECHANISM

In this section, the stable configurations for the averaged dynamics of the 2-link mechanism are determined for a range of values $r \in [0, 10]$ m/s with $\varepsilon = 1/70$ and $\psi = \frac{2\pi}{3}$ radians. The physical parameters of the nominal system are given in Table 1. Various stable configurations for the dynamics defined in (10)

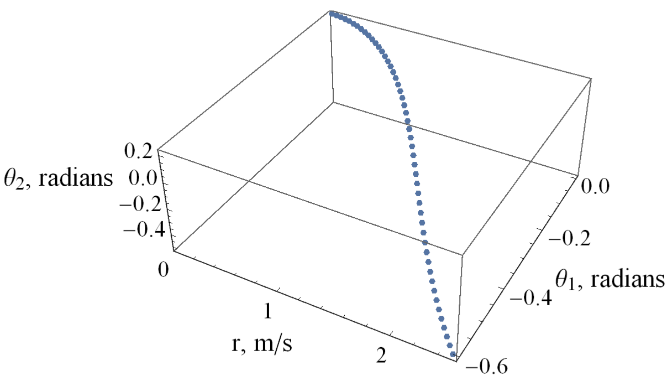

(a) STABLE CONFIGURATIONS (θ_1, θ_2) OF THE NOMINAL SYSTEM WITH VARYING r.

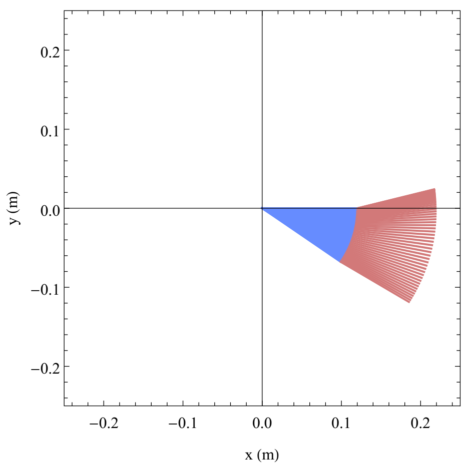

(b) DEPICTION OF STABLE CONFIGURATIONS OF THE NOMINAL SYSTEM. BLUE AND RED LINES REPRESENT LINKS 1 AND 2, RESPECTIVELY.

FIGURE 3: STABLE CONFIGURATIONS OF THE NOMINAL SYSTEM.

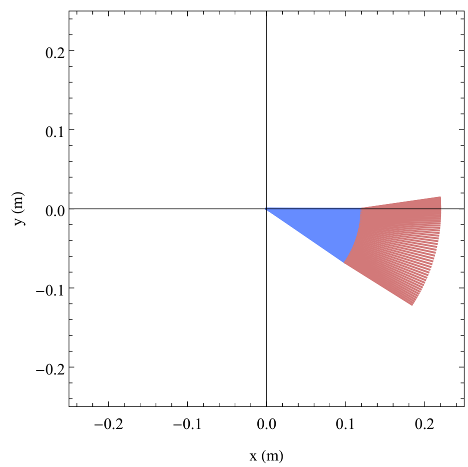

(a) $\gamma = \frac{1}{2}\gamma^0$.

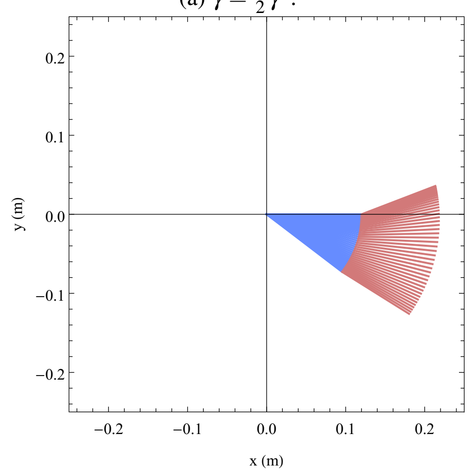

(b) $\gamma = 2\gamma^0$.

FIGURE 4: STABLE CONFIGURATIONS FOR DIFFERENT VALUES OF γ.

using the given parameter values are depicted in Fig. 3.

Effects of Parameters on Stable Configurations

To examine the effect of parameter values on the equilibria and their stability, we define the following non-dimensional parameters

$$\gamma = \frac{m_1}{m_2} \qquad \text{and} \qquad \lambda = \frac{l_1}{l_2}$$

We denote the nominal values, corresponding to the values in Table 1, with a superscript "0". The variations considered here are $\gamma \in \{\frac{1}{2}\gamma^0, 2\gamma^0\}$, $\lambda \in \{\frac{1}{2}\lambda^0, 2\lambda^0\}$, $k_{t_1} \in \{\frac{1}{2}k_{t_1}^0, 2k_{t_1}^0\}$, and $k_{t_2} =$ 0.25 N-m/rad. Fig. 4 indicates that when the mass of link 1 is larger than the mass of link 2, there are more achievable stable configurations over the range of r-values tested. The variation of the lengths of the links does not cause a noticeable difference in stable configurations, however, as seen in Fig. 5. Reducing the torsional stiffness applied at the base pivot as shown in Fig. 6a decreases the range of achievable stable configurations while increasing the torsional stiffness as in Fig. 6b increases the number of achievable stable configurations. Figure 7 presents the stable configurations when a non-zero value for the torsional stiffness in joint B, k_{t_2}, is introduced. Adding torsional stiffness to joint B causes the range of stability of the first link to increase. The second link stays more aligned with the first link due to the addition of the torsional stiffness in joint B.

The results of the parameter variation reveal the parameters that the system is most sensitive to. For the nominal system in this study, $\gamma = 1.2$. When designing an experiment to test this system, increasing the mass ratio γ will allow us to achieve a

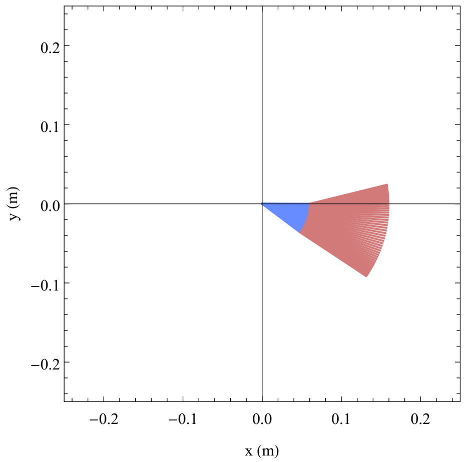

(a) $\lambda = \frac{1}{2}\lambda^0$.

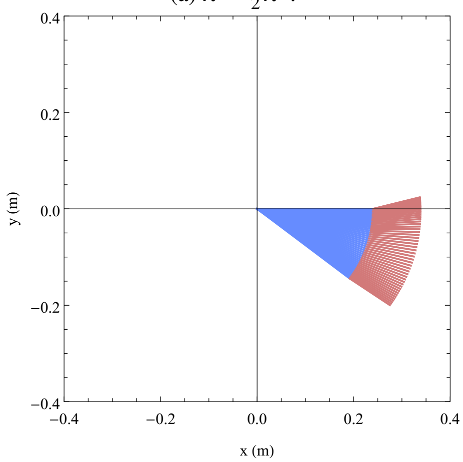

(b) $\lambda = 2\lambda^0$.

FIGURE 5: STABLE CONFIGURATIONS FOR DIFFERENT VALUES OF λ.

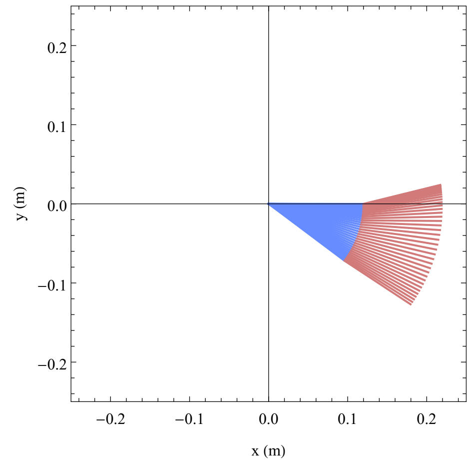

(a) $k_{t_1} = \frac{1}{2}k_{t_1}^0$.

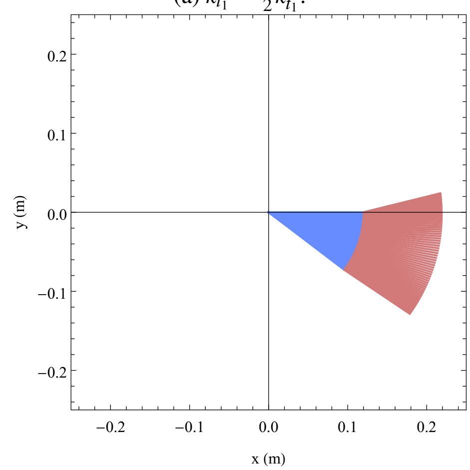

(b) $k_{t_1} = 2k_{t_1}^0$.

FIGURE 6: STABLE CONFIGURATIONS FOR DIFFERENT VALUES OF k_{t_1}.

wider range of stable configurations. The length of the system can vary without affecting the stable configurations, which allows for some freedom in the selection of the thicknesses and widths of the links to accommodate hardware such as bearings and torsional springs in the pivots. The results presented in this manuscript will be used to design a 2-link mechanism and explore the stable configurations while varying the amplitude of the periodic forcing.

STABILITY ANALYSIS USING AVERAGED POTENTIAL

In this section, we analyze stability using the *averaged potential* described by Weibel and Baillieul in [15]. Following the steps outlined in [15], we consider a Lagrangian of the form

$$L(\mathbf{q},\dot{\mathbf{q}};v) = \frac{1}{2}\dot{\mathbf{q}}^T\mathbf{M}(\mathbf{q})\dot{\mathbf{q}} + v\mathbf{a}^T(\mathbf{q})\dot{\mathbf{q}} - V(\mathbf{q};v) \qquad (12)$$

where $\mathbf{q} = (\theta_1, \theta_2)^T$, $\mathbf{M}(\mathbf{q})$ is the inertia matrix, v is the time derivative of the input, $R = r\varepsilon\cos\left(\frac{t}{\varepsilon}\right)$,

$$\mathbf{a}(\mathbf{q}) = \begin{pmatrix} -\left(d_1m_1 + l_1m_2\right)\sin\left(\theta_1 - \psi\right) \\ -d_2m_2\sin\left(\theta_2 - \psi\right) \end{pmatrix}$$

and

$$V(\mathbf{q};v) = \mathbf{q}^T\begin{pmatrix} k_{t_1} + k_{t_2} & -k_{t_2} \\ -k_{t_2} & k_{t_2} \end{pmatrix}\mathbf{q} - \frac{1}{2}(m_1 + m_2)v^2$$

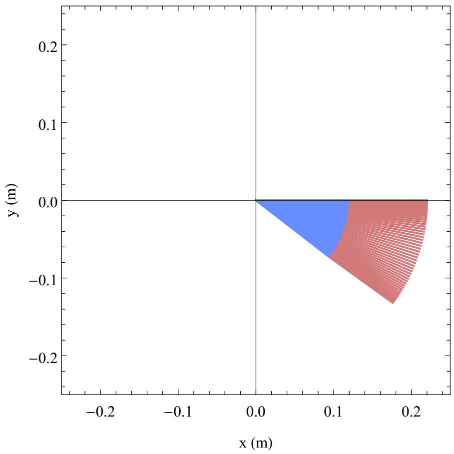

FIGURE 7: STABLE CONFIGURATIONS WITH $k_{t_2} = 0.25$ N-m/rad.

The Hamiltonian corresponding to this system is

$$H(\mathbf{q},\mathbf{p};v) = \frac{1}{2}(\mathbf{p}-v\mathbf{a})^T\mathbf{M}^{-1}(\mathbf{p}-v\mathbf{a}) + V \tag{13}$$

where $\mathbf{p}$ are the conjugate momenta to the generalized coordinates $\mathbf{q}$. We can apply simple averaging to the Hamiltonian in Eqn. (13) to obtain

$$\begin{aligned}\overline{H}(\mathbf{q},\mathbf{p}) &= \frac{1}{T}\int_0^T H(\mathbf{q},\mathbf{p};v)dt \\ &= \frac{1}{2}\mathbf{p}^T\mathbf{M}^{-1}\mathbf{p} - \overline{v}\mathbf{a}^T\mathbf{M}^{-1}\mathbf{p} + \frac{1}{2}\overline{v}\mathbf{a}^T\mathbf{M}^{-1}\mathbf{a}\overline{v} + \overline{V}\end{aligned} \tag{14}$$

where the overbar denotes a simple average. The input v is a zero-mean, T-periodic function, therefore its average $\frac{1}{T}\int_0^T v dt = 0$ and the term $\overline{v}\mathbf{a}^T\mathbf{M}^{-1}\mathbf{p} = 0$. The averaged Hamiltonian $\overline{H}(\mathbf{q},\mathbf{p})$ is divided into two parts: an averaged kinetic energy

$$T_{\mathrm{A}} = \frac{1}{2}\mathbf{p}^T\mathbf{M}^{-1}\mathbf{p} \tag{15}$$

and an averaged potential

$$V_{\mathrm{A}} = \frac{1}{2}\overline{(v^2)}\mathbf{a}^T\mathbf{M}^{-1}\mathbf{a} + \overline{V} \tag{16}$$

The equilibrium configurations $\mathbf{q}_*$ of the system are found by solving the following equation

$$\frac{\partial V_{\mathrm{A}}}{\partial \mathbf{q}}(\mathbf{q};r;\psi) = \mathbf{0} \tag{17}$$

for the roots $\mathbf{q} = \mathbf{q}_*$. The stability of each equilibrium for the T-averaged dynamics is determined by the eigenvalues of the Hessian matrix evaluated at the equilibrium:

$$\mathrm{Hess}\big(V_{\mathrm{A}}(\mathbf{q};r;\psi)\big)\big|_{\mathbf{q}=\mathbf{q}_*} = \left.\begin{pmatrix} \frac{\partial^2 V_{\mathrm{A}}}{\partial \theta_1^2} & \frac{\partial^2 V_{\mathrm{A}}}{\partial \theta_1 \partial \theta_2} \\ \frac{\partial^2 V_{\mathrm{A}}}{\partial \theta_1 \partial \theta_2} & \frac{\partial^2 V_{\mathrm{A}}}{\partial \theta_2^2} \end{pmatrix}\right|_{\mathbf{q}=\mathbf{q}_*}$$

For stability, the Hessian matrix must be positive definite. Equivalently, its eigenvalues must be positive. According to [15], stability of the equilibrium for the time-averaged system implies stability of the periodic orbit for the original time-varying system.

We consider the same desired equilibrium used in the result in Fig. 2, $\mathbf{q}_* = (-\frac{\pi}{18}, \frac{\pi}{9})^T$ radians, and solve for values of r and the angle ψ which will achieve the desired configuration of the links using Eqn. (17). This process gives the values $r_{\mathrm{e}} = 1.74$ m/s and $\psi_{\mathrm{e}} = 1.64$ radians. Evaluating the Hessian matrix at this desired equilibrium, with the given values r_{e} and ψ_{e}, one finds that it is positive definite, indicating that the desired equilibrium is stable. Applying similar analysis to the range of simulation results in the previous section confirms stability as indicated by the simulations. The two methods used to perform stability analysis provide the same results for a desired configuration of the 2-link mechanism.

CONCLUSION

This paper presented a numerical and analytical investigation of vibrational control of a 3-DOF planar, horizontal 2-link mechanism. The effects of varying the physical parameters of the system on the achievable stable orientations of the links were explored over a range of amplitudes of the vibrational input for a prescribed input angle and oscillation frequency. Stability analysis was performed for one particular equilibrium using the averaged dynamics and the averaged potential. The results of the stability analysis were the same for both methods. As future work, this system will be physically constructed and the achievable stable configurations of the physical system will be compared with the analytical results obtained following the procedure outlined in this paper. We will also endeavor to answer the questions posed in the introduction for a more general class of systems.

ACKNOWLEDGMENT

This research was supported by the National Science Foundation under Grant No. CMMI-1635143.

REFERENCES

[1] Meerkov, S. M., 1977. "Vibrational Control Theory". *Journal of the Franklin Institute,* ***303***(2), February, pp. 117–128.

[2] Bellman, R. E., Bentsman, J., and Meerkov, S. M., 1986. "Vibrational Control of Nonlinear Systems: Vibrational Stabilizability". *IEEE Transactions on Automatic Control*(8), August, pp. 710–716.

[3] Bellman, R. E., Bentsman, J., and Meerkov, S. M., 1986. "Vibrational Control of Nonlinear Systems: Vibrational Controllability and Transient Behavior". *IEEE Transactions on Automatic Control,* ***31***(8), August, pp. 717–724.

[4] Guckenheimer, J., and Holmes, P., 1983. *Nonlinear Oscillations, Dynamical Systems, and Bifurcations of Vector Fields*. Springer-Verlag, New York, NY.

[5] J.A. Sanders, F. V., and Murdock, J., 2007. *Averaging Methods in Nonlinear Dynamical Systems*. Springer-Verlag, New York, NY.

[6] Bogoliubov, N., and Mitropolsky, Y., 1961. *Asymptotic Methods in the Theory of Nonlinear Oscillations*. Hindustan Publishing Corporation, Delhi.

[7] Bullo, F., 2002. "Averaging and Vibrational Control of Mechanical Systems". *SIAM Journal on Control and Optimization,* ***41***(2), June, pp. 542–562.

[8] Bullo, F., and Lewis, A., 2005. *Geometric Control of Mechanical Systems*. Springer, New York, NY.

[9] Tahmasian, S., and Woolsey, C., 2015. "A Control Design Method for Underactuated Mechanical Systems Using High-Frequency Inputs". *ASME Journal of Dynamic Systems, Measurement, and Control,* ***137***(7), July, pp. 071004: 1–11.

[10] Tahmasian, S., Jafari, F., and Woolsey, C., 2016. "On vibrational stabilization of a horizontal pendulum". In Proceedings of the ASME 2016 Dynamic Systems and Control Conference, ASME, pp. 1–10. Paper Number DSCC2016-9675.

[11] Vela, P., Morgansen, K., and Burdick, J., 2002. "Second order averaging methods for oscillatory control of underactuated mechanical systems". In Proceedings of the 2002 American Control Conference, Vol. 6, IEEE, pp. 4672–4677.

[12] Morgansen, K., Vela, P., and Burdick, J., 2002. "Trajectory stabilization for a planar carangiform robot fish". In Proceedings of the 2002 IEEE International Conference on Robotics and Automation, Vol. 1, IEEE, pp. 756–762.

[13] Berg, J. M., and Wickramasinghe, I., 2015. "Vibrational control without averaging". *Automatica,* ***58***(2015), April, pp. 72–81.

[14] Baillieul, J., 1995. "Energy Methods for Stability of Bilinear Systems with Oscillatory Inputs". *International Journal of Robust and Nonlinear Control,* ***5***, pp. 285–301.

[15] Weibel, S., and Baillieul, J., 1998. "Averaging and energy methods for robust open-loop control of mechanical systems". In *Essays on Mathematical Robotics*, J. Bailliuel, S. S. Sastry, and H. J. Sussman, eds., Vol. 104 of *IMA Volumes in Mathematics and its Applications*. Springer-Verlag, New York, pp. 1–3.

[16] Wickramasinghe, I., and Berg, J., 2013. "Delay of side pull-in for an electrostatic comb drive model with rotational degree of freedom". In American Control Conference, pp. 6251–6256.

[17] Taha, H., Kiani, M., and Navarro, J., 2018. "Vibrational Control in Flapping-Wing Micro-Air-Vehicles". In American Control Conference, pp. 6445–6450.

[18] Guo, Y., Wang, Z., Qu, Z., and Braiman, Y., 2011. "Atomic-scale friction control by vibration using friction force microscope". *Control Engineering Practice,* ***19***(11), November, pp. 1387–1397.

[19] Blekhman, I. I., 2007. *Vibrational Mechanics - a General Approach to Solving Nonlinear Problems*. Springer Vienna, Vienna.

[20] Tahmasian, S., Allen, D., and Woolsey, C., 2016. "On averaging and input optimization of high-frequency mechanical systems". *SAGE Journal of Vibration and Control,* ***24***(5), July, pp. 937–955.